THE ASTROPHYSICAL JOURNAL, 447:752–759, 1995 July 10

VLBI OBSERVATIONS OF CYGNUS X-3 DURING THE 1985 OCTOBER RADIO OUTBURST

C. J. SCHALINSKI,[1,2,3] K. J. JOHNSTON,[4] A. WITZEL,[1] R. E. SPENCER,[5] R. FIEDLER,[6] E. WALTMAN,[6]
G. G. POOLEY,[7] R. HJELLMING,[8] AND L. A. MOLNAR[9]
Received 1992 June 29; accepted 1994 July 18

ABSTRACT

Cygnus X-3 underwent a large outburst beginning on 1985 October 2 and reached a peak flux density of 18 Jy at 11.1 cm on October 10. Between October 7 and October 19 we performed seven snapshot observations at a wavelength of 6 cm using telescopes of the European VLBI Network. The source structure may be represented by three components, consistent with a pair of symmetrical jets emanating from a central compact object. The component sizes are consistent with broadening by interstellar scattering to 16 ± 6 mas. Comparison with other data shows that the frequency dependence of the scattered image varies as $\nu^{-2.07\pm0.04}$ and that the scattering toward Cygnus X-3 is enhanced compared with other Galactic sources. We estimate that the emission in the symmetrical components has an apparent proper motion of 4.2 mas day^{-1} or $0.3c$ at a distance of 10 kpc. Study of the VLBI structure and total flux density variability yields an upper limit for the distance to Cygnus X-3 of 15 kpc.

Subject headings: binaries: close — ISM: jets and outflows — stars: individual (Cygnus X-3) — X-rays: stars

1. INTRODUCTION

Since the discovery of a giant outburst of the radio counterpart to the X-ray source Cygnus X-3 in 1972 September (Gregory et al. 1972), intensive coordinated monitoring programs at frequencies from radio to X-rays have led to the following interesting results.

A 4.8 hr periodicity has been established from both the X-ray (Brinkman et al. 1972) and IR data (Becklin et al. 1972). This is interpreted as the orbital period of a binary system with mass transfer from a star which fills its Roche lobe onto a compact companion (Davidsen & Ostriker 1974; van den Heuvel & De Loore 1973). Interstellar extinction of 19 visual mag prevents an optical identification (Weekes & Geary 1982), and only a lower distance limit of about 10 kpc is derived from H I absorption-line measurements (Dickey 1983).

The radio emission can be described as a superposition of individual flares which differ by two orders of magnitude in intensity and have timescales of hours to weeks (Johnston et al. 1986). In addition to the large outbursts, the quiescent state of the source has been shown to consist of "mini"-flares of order 100 mJy (Molnar, Reid, & Grindlay, 1984; Molnar, Reid, & Grindlay 1985).

The 1972 September outburst can be characterized by synchrotron and adiabatic losses from a uniformly expanding cloud of relativistic particles and magnetic fields which are mixed with an ionized thermal plasma (Marscher & Brown 1975). VLA measurements by Geldzahler et al. (1983) at 1.3, 2, and 20 cm of a large flaring event which occurred in 1982 October showed that the source became resolved 21 days after the outburst. An apparent expansion rate of 0".01 day^{-1} along a position angle (p.a.) of 0° was estimated. MERLIN observations at 6 cm by Spencer et al. (1986) in 1983 October of another large flaring event showed that the radio emission became resolved and expanded to a maximum size of 77 mas along the same position angle, giving an expansion rate in the range of 5–18 mas day^{-1}.

In order to investigate details of the kinematics, the spatial structure close to the source of the outbursts must be mapped; this makes it necessary to carry out high-resolution (VLBI) measurements during a flaring event. However, three problems have to be considered: first, aperture synthesis observations of flaring events prevent the application of standard mapping techniques due to flux density variations during an observation; second, any expansion model depends on the identification of the initial onset of a particular outburst; and third, even though the occurrence of an outburst detected by flux density monitoring can be reported immediately, scheduling VLBI runs on an ad hoc basis, even during regular network sessions, is a major problem.

In this paper, we report on monitoring observations of the outburst of 1985 October made with the Green Bank interferometer at wavelengths of 11 and 3.7 cm; the Effelsberg telescope at 6 cm; the Cambridge 5 km telescope at 6 cm; and the VLA at 20, 6, 2, and 1.3 cm. Snapshot VLBI observations were obtained with telescopes of the European VLBI Network (EVN) at a wavelength of 6 cm. VLBI observations at 6 cm during a quiescent phase in 1985 May are also reported for comparison.

2. OBSERVATIONS AND DATA REDUCTION

2.1. *Flux Density Observations*

The Green Bank interferometer monitors the flux densities of Cygnus X-3 at 11.1 and 3.7 cm in two circular polarizations 3 times a day using a baseline length of 2.4 km. Each obser-

[1] Max-Planck-Institut für Radioastronomie, Auf dem Hügel 69, D-53121 Bonn, Germany.
[2] Geodätisches Institut, University of Bonn, Nußallee, D-53121 Bonn, Germany.
[3] Present address: Institut für Weltraum Sensorik (DLR) Berlin, Germany.
[4] US Naval Observatory, 3450 Massachusetts Avenue, NW, Washington, DC 20392-5420.
[5] University of Manchester, Nuffield Radio Astronomy Laboratories, Jodrell Bank, Macclesfield, Cheshire SK11 9DL, England.
[6] Naval Research Laboratory, Code 7200, Remote Sensing Division, Washington, DC 20375-5351.
[7] University of Cambridge, Institute of Astronomy, The Observatories, Madingley Road, Cambridge CB3 0HA, England.
[8] National Radio Astronomy Observatory, P.O. Box O, Socorro, NM 87801.
[9] University of Iowa, Department of Physics and Astronomy, 203 Van Allen Hall, Iowa City, IA 52242.

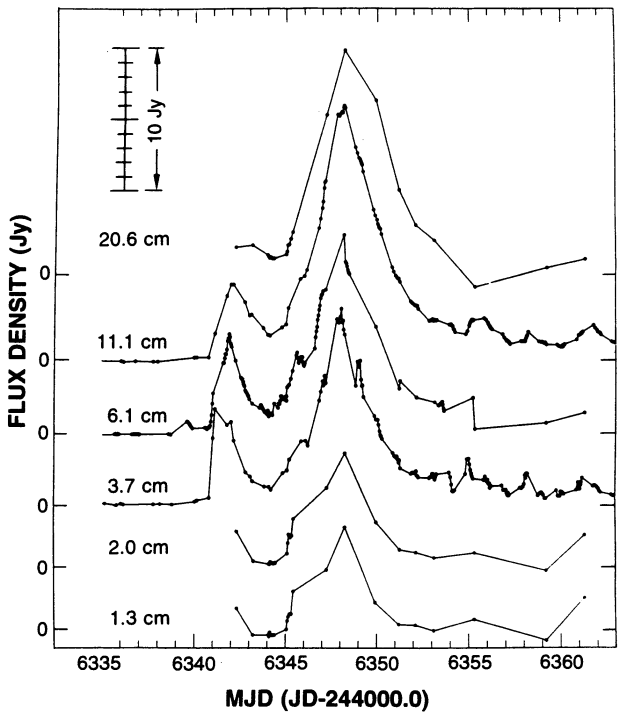

FIG. 1.—The flux density variations of Cygnus X-3 in 1985 October as observed with the Green Bank interferometer at 11.1 and 3.7 cm, the Effelsberg telescope at 6 cm, the Cambridge 5.1 km telescope at 6 cm, and the VLA at 20, 6, 2, and 1.3 cm. Note that the more frequently sampled wavelengths at 11.1, 6.1, and 3.7 cm display a great deal of fine-scale variations of less than a day. The solid lines connecting the data points are meant only as aids in following the light curves.

vation was 10 minutes long with the two wavelengths being alternated every 30 s. The flux density scale is based on 3C 286, which is assumed to have a flux density of 10.5 and 5.3 Jy at 11.1 and 3.7 cm, respectively. The rms of a single observation is of order 50 and 80 mJy at 11.1 and 3.7 cm. For more details of the instrument and the calibration of these observations, see Johnston et al. (1986) and Fiedler et al. (1987). An increase of flux density to over 7 Jy at a wavelength of 3.7 cm was observed on 1985 October 3. Subsequently, the flux density of Cygnus X-3 was monitored 8 times a day until the flux density decreased to less than 1 Jy. The resulting light curve of Cygnus X-3 in left circular polarization is shown in Figure 1.

From Figure 1, it can be seen that the initial flare which occurred on October 3 was followed by a large flare about 7 days later, reaching a peak flux density of about 18 and 14 Jy at 11.1 and 3.7 cm, respectively. This large flare was followed by several weaker flares of the order of 2–3 Jy at 7, 10, and 14 days after the time of peak flux density. The peak intensities and the estimated initial time of the flaring events are given in Table 1.

Flux density measurements were obtained with the Cambridge 5 km telescope at 6 cm around the date of the initial flare and with the VLA and Effelsberg telescopes after the initial flare was detected by the Green Bank Interferometer. Measurements were obtained using the Effelsberg 100 m telescope at 6 cm and the VLA[10] at wavelengths of 20, 6, 2, and 1.3 cm. The Cambridge and Effelsberg measurements are also

[10] The VLA is a telescope of the National Radio Astronomy Observatory which is operated by Associated Universities Inc. under contract with the National Science Foundation.

TABLE 1

FLARING EVENTS FOR CYGNUS X-3 IN 1985 OCTOBER

DATE (1985)	JULIAN DATE	PEAK FLUX DENSITY (Jy) $\lambda = 11.1$ cm	PEAK FLUX DENSITY (Jy) $\lambda = 3.7$ cm
Oct 3.....	2,446,341.68	5.5	6.9
Oct 10.....	2,446,348.54	18.4	14.0
Oct 16.....	2,446,355.45	3.7	3.7
Oct 19.....	2,446,358.68	2.5	2.5
Oct 22.....	2,446,361.81	2.8	1.5

shown in Figure 1 and contain frequent enough sampling to give a good representation of the light curve of this event. The rms errors of these observations are less than a few percent of the observed flux density. The flux densities at 6.1 cm, obtained with the VLA, the Cambridge, and the Effelsberg telescopes, agree within the errors for the measurements, which were taken quasi-simultaneously. The VLA data sampled the flux density variability at less frequent intervals but are extremely useful for determination of representative spectral indices of the emission. The VLA data are also shown in Figure 1.

2.2. *VLBI Observations*

The EVN is a sensitive network comprising the following telescopes: Effelsberg (100 m), Westerbork (WSRT) (22 × 25 m), Medicina (32 m), Jodrell Bank (25 m), and Onsala (25 m). Baselines range from about 270 km (Effelsberg-WSRT) to about 1400 km (Medicina-Onsala), corresponding to angular resolutions between 26 and 5 mas at 6.1 cm.

The initial outburst observed with the Green Bank interferometer on 1985 October 2 prompted us to organize an ad hoc VLBI experiment which used every gap between scheduled projects of the 1985 October European VLBI network run. Between October 7 and 19 we obtained observations of 1–8 hr at seven epochs.

The data were taken at a center frequency of 4991.99 MHz (6 cm wavelength) using the Mk II system at a bandwidth of 2 MHz. The observations were performed in 30 minute scans to allow for sufficient system calibration at each telescope and, in the cases where Effelsberg took part, to provide flux density monitoring of the source.

The correlation and postprocessing of the data were performed at the processing center of the MPIfR, Bonn. Coherence tests allowed an integration time of 240 s (<5% coherence losses). The amplitude calibration was initially done using the reported system temperatures and gain curves of the telescopes. The gain curves were obtained from observatory reports and have estimated accuracies of 5%–10%.

Amplitude calibration was obtained from model-fitting sources of adjacent VLBI observations and also model fits from occasional observations of the unresolved source 2005+403 (2.5 ± 0.3 Jy at 6 cm determined from 100 m observations). The calibration file obtained by this procedure was then used to calibrate the visibility amplitudes of the Cygnus X-3 data. In order to improve the quality of the data and especially to reduce the noise of the closure phases, we applied a global fringe-fitting algorithm (Alef & Porcas 1986) to those data which were taken with at least three telescopes.

In addition to the observation of the large flare in 1985 October, VLBI snapshot observations using the wide-band MKIII recording system were made earlier on 1985 May 21 and 23 at 0440 UT during a quiescent phase of Cygnus X-3.

Thirteen minute observations were taken with the European VLBI Network at a center frequency of 4985 MHz (6 cm wavelength) with a 56 MHz bandwidth using the Effelsberg, Westerbork, Medicina, and Onsala telescopes. The data were also processed at MPIfR, Bonn, and calibrated using the given system temperatures and adjacent observations of 2005+403. Measurements with the Effelsberg telescope indicated a total flux density of 4.0 ± 0.1 Jy for 2005+403. Comparison with the flux density obtained at the same frequency during the 1985 October run indicates variability of the source, which is not unusual for quasars in general. Given that these observations were obtained within 6 months of each other, the variability would likely be unresolved at our frequency and fringe spacings. Odd fringes on the calibrator consistent with this flux density were detected on all baselines, but Cygnus X-3 was detected on only the shortest baselines, Effelsberg-Westerbork, at flux density levels of 59 ± 6 and 50 ± 6 mJy on May 21 and 23, respectively. Upper limits range from 7 to 40 mJy (6 σ) on the longer baselines indicating that Cygnus X-3 was resolved with the most useful limit being set by the Effelsberg-Medicina baseline at 7 mJy (see discussion in next section).

3. RESULTS

The radio light curve of 1985 October shows that the flux density outburst occurred with at least five major components: October 3, 10, 16, 19, and 22. We note that the large flare which occurred after the initial flare quickly became optically thin as can be seen from inspection of the 11.1 and 3.7 data in Figure 1 and showed the same characteristics as the flaring events which occurred in the 1972 events (Gregory et al. 1972). The radio emission was particularly weak ($\leq$50 mJy) on the day immediately preceding the initial flare on October 3.

Fringes were detected on October 7, 9, 10, 12, 13, 15/16, and 19. Although the flux density of Cygnus X-3 was on the order of 10 Jy, it was heavily resolved over the EVN baselines. The correlated flux densities were less than 0.5 Jy except on the shortest baseline, Effelsberg-WSRT. Only those baselines to the 100 m telescope had sufficient sensitivity to allow for a detailed reconstruction of the source structure. The Effelsberg telescope could be included in the observations on only October 10 and 15/16. Figure 2 shows the correlated flux densities as a function of interferometer hour angle.

With this limited data set of visibility amplitudes and phases, the CalTech model fit program was employed to ascertain the structure of Cygnus X-3. The visibility amplitude (epoch October 15/16) of the Effelsberg-Medicina baseline, which is almost north-south, is indicative of a linear structure with a p.a. of 180°. Obviously there exists a variety of models, each of which fits the data within the errors. We performed many tests using the "grid-fit" mode of the CalTech model-fitting routine. All parameters with the exception of the position of the central component were allowed to vary. Only those solutions were accepted which were "stable" (after repeated iterations) and which gave a good fit to the data. The only physical boundary condition was the total flux density of Cygnus X-3 at the epoch of the VLBI observations.

The results of these model fits are presented in Table 2. Column (1) lists the component flux densities S, in Jy; column (2), the radius, r, is the component separation in milliarcseconds with respect to the origin; column (3), θ, is the component position angle with respect to the origin in degrees (counterclockwise from the north); columns (4) and (5) are the major and minor axes of the elliptical component in milliarcseconds; and column (6) is the position angle Φ of the major axis in degrees.

The errors for the parameters listed in Table 2, derived from multiple model fits to the data, are ±10% or at least 0.1 Jy for the flux densities, ±4 mas for the separation, ±30° for the corresponding p.a.'s, and ±2–10 mas for the component diameters. In particular the real diameters of the secondary components might be underestimated due to the resolution effects mentioned above.

Neither a one-component model nor a two-component model (two similar components or a compact component plus an elongated halo) fulfilling the above criteria could be fitted to the October 15/16 data, so that a three-component model is the least complex representation of the source structure (Fig. 3*c*). Thus, the structure on October 15/16 appears to consist of

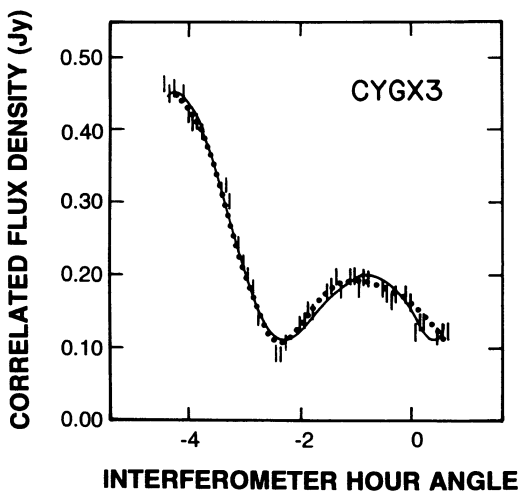

FIG. 2*a*

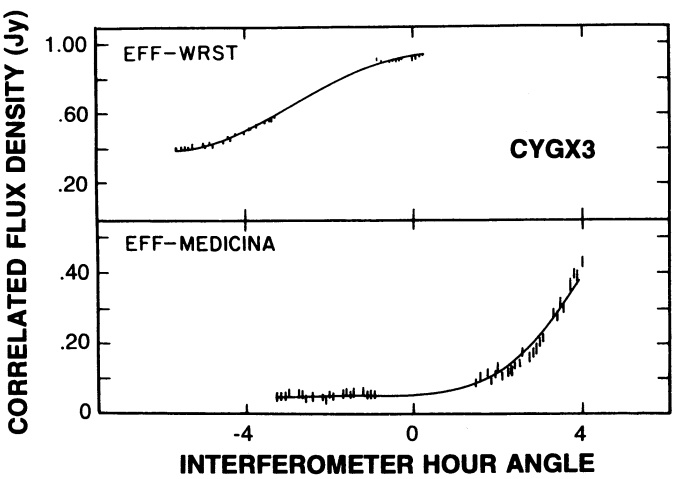

FIG. 2*b*

FIG. 2.—(*a*) The solid line represents the predicted visibility of a double-source model, while the dotted line represents a triple-source model with component parameters given in Table 2. (*b*) Cross-correlated flux density on the baselines Effelsberg to Westerbork and Effelsberg to Medicina for October 15/16. Again the solid curve is a model fit with the parameters given in Table 2.

TABLE 2

MODEL FITS TO THE CYGNUS X-3 6 CENTIMETER VLBI DATA

Flux Density (Jy) (1)	Radius (mas) (2)	θ (3)	Major Axis (mas) (4)	Minor Axis (mas) (5)	Φ (6)
1985 October 10: Two-Component Model					
9.6 ± 0.9	0	0°	28 ± 10	15 ± 5	68°:
1.0 ± 0.3	31 ± 5	181 ± 30	24 ± 10	≤ 24	...
1985 October 10: Three-Component Model					
9.9 ± 0.9	0	0°	19 ± 4	17 ± 2	76°:
0.47 ± 0.1	28 ± 4	7 ± 30	24 ± 10	≤ 24	...
0.49 ± 0.1	30 ± 4	169 ± 30	34 ± 10	≤ 34	...
1985 October 15/16: Three-Component Model					
0.98 ± 0.15.....	0	0°	20 ± 3	14 ± 1	77°:
0.46 ± 0.11.....	32 ± 4	24 ± 30	34 ± 6	≤ 34	...
0.29 ± 0.12.....	29 ± 4	211 ± 30	29 ± 6	≤ 29	...

a compact 16 mas core and two secondary 30 ± 5 mas components on either side with a separation of 30 ± 5 mas at a p.a. of $30° \pm 20°$. The VLBI components account for the total flux density within the errors. Less than 20% of the total flux density at 5 GHz is distributed over an extended region resolved out by these measurements, which implies that no larger, unresolved component exists.

Because of sensitivity problems and telescope failures on October 10, only the Effelsberg-Medicina baseline could be used for the analysis (Fig. 2*a*). The simplest model which fits the data consists of two components separated by 31 mas at a p.a. of 181° (Fig. 3*a*). The component flux densities (Table 2) add up to the total flux density of 11.6 Jy within the errors, again indicating that no larger, unresolved component is present. Component separation and p.a. are well defined by the minimum on the Effelsberg-Medicina baseline. However, a three-component model with two components on opposite sides, but with the same separation and small flux density ratios with respect to the central component, results in a similar one-baseline fit (Fig. 3*b*). The corresponding numbers are also given in Table 2. Within the modeling errors, the orientation of the components is the same in Figures 3*a*, 3*b*, and 3*c*.

Although a variety of possible solutions exists which match the data, the parameters of the two-component model of October 10 in Table 2 put constraints on more complex models. First, the overall size of the structure is limited to 2 times 30 mas (and defines an upper limit to the expansion velocity), and the p.a. must be on the order of 180°. Second, the structure during the outburst is dominated by the compact component; the size of this component should be comparable to the corresponding value from the two-component model. The best three-component model is presented in Figure 3*b*, and the source parameters are listed in Table 2. The core-flux densities of the October 10 models agree within 5% and are a factor 10 above the flux density of the October 15/16 "core." The core of model 1 (October 10) is elongated and less compact than the secondary components. We adopt the weighted geometric mean of the major and minor axes of the dominant compact component determined from the three model fits listed in Table 2, 16 ± 6 mas, as the relevant size of the compact component of Cygnus X-3.

Although the October 10 data consist of only one baseline (Effelsberg-Medicina), the pronounced minimum in the visibility amplitude allows us to determine a well-defined p.a. of the relative position of the components. This position angle is consistent with results from lower resolution data (e.g., Spencer et al. 1986), whereas the p.a. is less well defined on the basis of the October 15/16 data. The errors from the model fits show that the parameters of the three-component models are consistent and indicate that this is probably a good representation of the milliarcsecond structure of Cygnus X-3 at 6 cm.

An estimate of the angular size of Cygnus X-3 during its quiescent phase can be made from the fringe visibilities on May 21 and 23. The total flux density at 6 cm was estimated to be 0.13 ± 0.01 Jy on these dates by interpolation from Green Bank Interferometer data at 2.7 and 8.1 GHz. An equivalent Gaussian width (FWHM) of 23 ± 2 mas, measured along a p.a. ~ 0, reproduced the observed fringe amplitudes. This is within the error bars of the sizes of the dominant compact component listed in Table 2.

We have not attempted to account for flux density variations in these model fits to the data. If we consider that the source is dominated by structures greater than 16 mas and that these structures are varying less than 20% in intensity during the observing periods, then the model fits derived above should be a good representation of the source structure.

4. DISCUSSION

4.1. *Interstellar Scattering toward Cygnus X-3*

Compared to the highest angular resolution of the EVN, 5 mas at 6 cm, the measured size of the compact component of Cygnus X-3, 16 ± 6 mas, is significantly extended. This size is listed in Table 3, along with earlier measurements by Anderson et al. (1972) and Wilkinson, Spencer, & Nelson (1988) at 73 cm, Geldzahler et al. (1983) at 20 cm, and Spencer et al. (1986) at 20 cm and 18 cm. A least-squares power-law solution gives $\delta = 2.07 \pm 0.04$, where $\theta \propto \nu^{-\delta}$ (see Fig. 4). This is in excellent agreement with the MERLIN observations at 73 cm by Wilkinson et al. (1988), who estimate the index to be $\delta = 2.08 \pm 0.03$.

This ν^{-2} dependence of source size is consistent with radio wave–scattering models based on the small-scale electron density turbulence in the interstellar medium (ISM). The power-law index β of the electron density irregularity spectrum

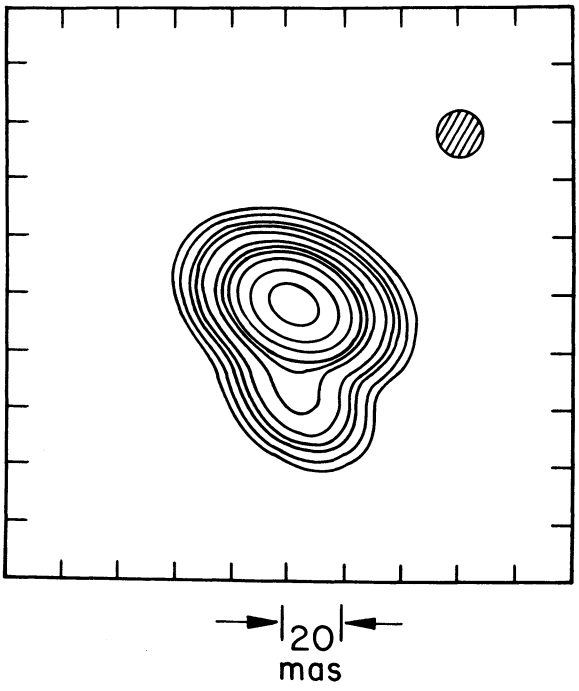

FIG. 3a

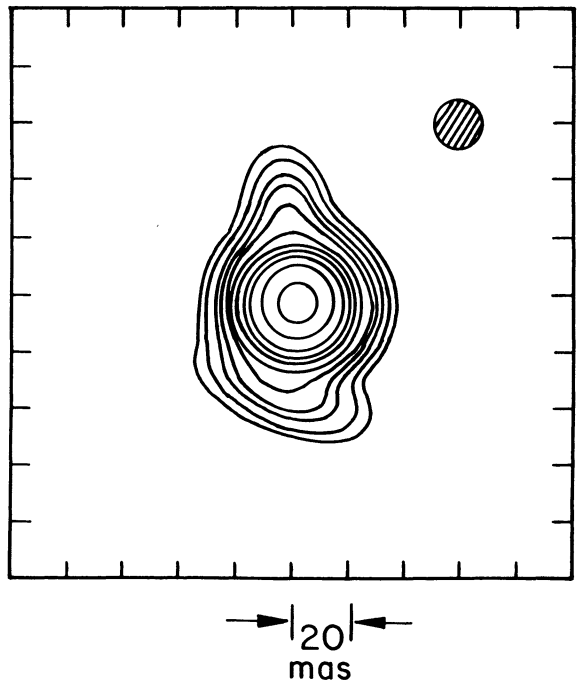

FIG. 3b

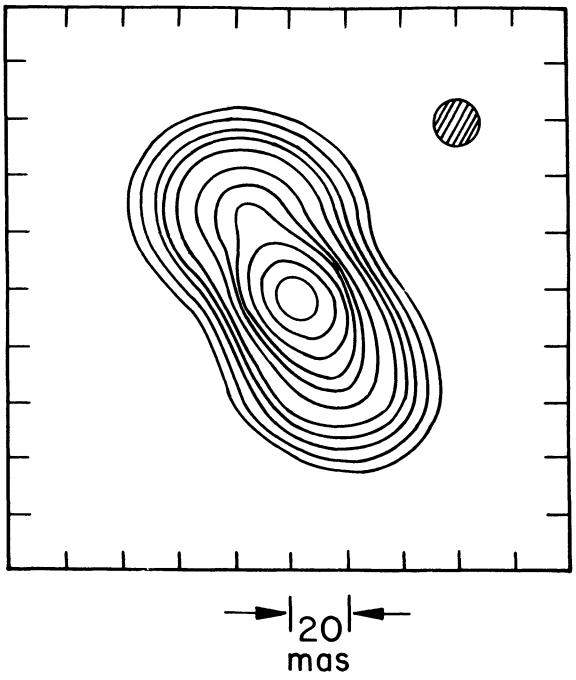

FIG. 3c

FIG. 3.—Model fit to visibility amplitude and closure phases. (*a*) Double-source model for October 10. (*b*) Triple-source model for October 10. (*c*) Model for October 15/16. The restoring beam is given as the cross-hatched area.

can be deduced from angular size measurements, since $\delta = \beta/(\beta - 2)$ (Cordes, Pidwerbetsky, & Lovelace 1986). Our results give $\beta = 3.87 \pm 0.07$, in good agreement with Wilkinson et al. (1988) who found $\beta = 3.88 \pm 0.05$ from the variation of visibility with baseline length at a single frequency. The turbulent wavenumber spectrum is usually expressed in the form $C_n^2 q^{-\beta}$, where C_n^2 is a measure of the strength of the fluctuations in the spatial wavenumber q. (Cordes et al. 1986). For reference, $\beta = 4$ represents a transition from diffractive- ($\beta < 4$) to refractive- ($\beta > 4$) dominated scattering. Also note that $\beta = 11/3$ corresponds to the Kolmogorov cascade of length scales. Although there is considerable interest in determining the characteristic value of β for the ISM, there has appeared in the literature a wide range, $2 < \beta < 4$, in the observed index with no evidence based on scattered images for values greater than 4.

A measure of the level of turbulence, $\langle C_n^2 \rangle$, over an effective path length, $L_{\rm kpc}$, is

$$\langle C_n^2 \rangle L \approx (\theta_{\rm max}/0.133)^{5/3} \nu_{\rm GHz}^{11/3} \approx 10.7_{\rm kpc\ m^{-20/3}} \quad (1)$$

from Cordes, Ananthakrishnan, & Dennison (1984).

These estimates for the power-law index and level of turbulence assume scattering from a plane wave source and a single-component irregularity wavenumber spectrum that is spatially uniform (Cordes, Weisberg, & Boriakoff 1985). Since any of these assumptions could easily be violated along the line of sight toward Cygnus X-3, the estimates should be interpreted

TABLE 3

SCATTERING SIZES VERSUS FREQUENCY

ν (GHz)	Φ	References
0.408.....	2.″7 ± 0.″3	1
0.408.....	2.85 ± 0.05	2
1.465.....	0.24 ± 0.2	3
1.465.....	0.23 ± 0.14	4
1.66.....	0.154 ± 0.01	4
1.66.....	0.22 ± 0.07	4
5.0.....	0.016 ± 0.006	5

REFERENCES.—(1) Anderson et al. 1972; (2) Wilkinson et al. 1988; (3) Geldzahler et al. 1983; (4) Spencer et al. 1986; (5) this work.

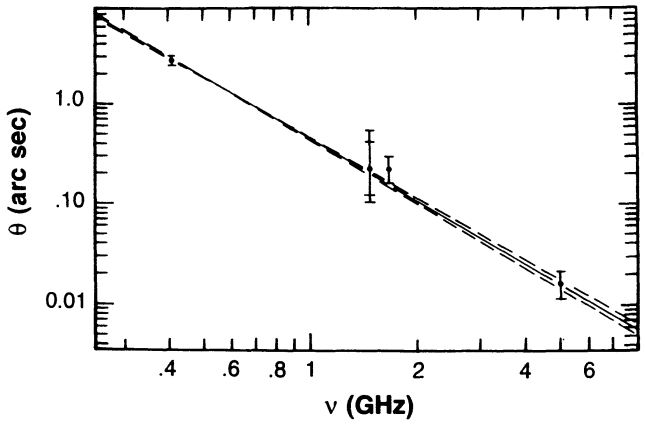

FIG. 4.—The reported minimum sizes for Cygnus X-3 as a function of frequency ν. The frequency dependence of the sizes as shown by the solid line is $\theta \approx \nu^{(-2.07 \pm 0.04)}$.

as a broad reference point when making comparisons with similar quantities along neighboring directions through the ISM. With this in mind, if we adopt an effective path length to Cygnus X-3 of 10 kpc, we find that this value for $\langle C_n^2 \rangle$ is nearly three standard deviations above the mean for pulsars within 5° of the plane (Cordes et al. 1985). Although our value for $\langle C_n^2 \rangle$ is probably an overestimate, the line of sight toward Cygnus X-3 evidently has enhanced turbulence.

A large scattering size, however, is not unusual for sources at low Galactic latitudes ($b <= 1°$). From VLBI observations of OH/H_2O maser sources in the Galactic plane, Diamond et al. (1988) and Gwinn et al. (1988) find evidence for a correlation of angular size with distance. The Cygnus region is particularly active, with high optical extinction and strong scattering, and may be located near regions of high energy input into the ISM (Cordes et al. 1985).

4.2. *Kinematics and Physical Parameters of Components*

The data of October 15/16 show that the source evolved from a compact source to one which is well represented by a triple with an angular extent of approximately 60 mas along a p.a. of 30° ± 20°. Thus the data are consistent with the assumption of two components moving out from a compact central component. If the outer double components are also assumed to have evolved from the maximum flux density outburst which occurred on October 10.0 (timescale 5.9 days), the expansion rate of these components is 5.1 ± 1.1 mas day^{-1} each, or a total source expansion rate of 10.2 mas day^{-1}. This translates into a velocity for the individual jetlike components of 0.29 ± 0.06c at a distance of 10 kpc. The observed sizes of the jet components imply a transverse expansion velocity of about 50% of this.

Although the October 10 data are sparse, we may use them to derive an upper limit on a possible expansion rate. Inspection of Figure 1 reveals a flare of order 6 Jy on October 3. If we assume that the structure observed on October 10 (three-component model in Table 2: median: 29 ± 6 mas) was the result of the flare on October 3, then a velocity estimate of $v = 0.32 \pm 0.08c$ results (6.9 days, i.e., 4.2 ± 1.2 mas day^{-1}). The three-component model indicates that only a small fraction of the flux density of October 10 (8%) is contained in the secondary components and that the structure is dominated by the large outburst of the compact component. If we assume that the structure observed on October 15/16 is the result of the flare on October 10, this yields a velocity of 0.37 ± 0.1c.

Previous estimates of the total source expansion were 10 ± 2 mas day^{-1} along a p.a. of 0° for the outburst of 1982 (Geldzahler et al. 1983) and about 12 mas day^{-1} along p.a. of 0° for the 1983 outburst (Spencer et al. 1986).

From observations at 1.3 cm during quiescent periods of Cygnus X-3, Molnar, Reid, & Grindlay (1988) estimate an expansion rate in the range of 0.16c–0.31c. Such expansion may be also taking place during our observations and may explain the extended core that we observe. There is therefore now good evidence for jetlike expansion from Cygnus X-3 at velocities of $0.3c \times d_{10\,\mathrm{kpc}}$.

The kinematic model also accounts for the nondetection on the baselines between Westerbork, Jodrell Bank, and Medicina on October 19. The secondary components are fully resolved, and an upper 7 σ limit of 200 mJy can be placed on the flux density of a compact component.

The observed velocity of $\beta_{\mathrm{obs}} = 0.3$ and the flux density ratio $R = 1.6$ of the secondary components of the October 15/16 model enables a rough estimate of the geometry to be made.

The minimum true velocity β_{min} is

$$\beta_{\mathrm{min}} = \beta_{\mathrm{obs}}(1 + \beta_{\mathrm{obs}}^2)^{-1/2} = 0.29$$

but

$$\beta \cos \Phi = (R^{1/3} - 1)/(R^{1/3} + 1)\,,$$

where $R = S_{\mathrm{jet}}/S_{\mathrm{counterjet}} = 1.6$, Φ minimum angle to the line of sight, and we assume the spectral index of 0 as an extreme case.

We thus obtain a minimum angle to the line of sight Φ in the range from 86° ($\beta_{\mathrm{max}} = 1$) to 74° ($\beta_{\mathrm{min}} = 0.29$). An angle to the line of sight of $\Phi = 74°$ gives no contradiction to the observed symmetry of antiparallel jets, because the deprojected size and projected size differ by only 2 mas, which is much smaller than the errors of component sizes and separations (Table 2).

Furthermore, the value of the largest deviation from the source structure oriented in the plane of the sky (about 26°) (Fig. 3c) is within the errors of the p.a. measurements (30°). Similar deviations can be measured from the observations on larger scales, e.g., by Spencer et al. (1986) and Strom, van Paradijs, & van der Klis (1989). This indicates good alignment of the structures on different scales even at different epochs (i.e., outbursts) and puts constraints on a possible misalignment caused by precession.

The brightness temperatures for the secondary components are on the order of 10^7 K with luminosities of order $10^{32}(d_{10\,\mathrm{kpc}})^2$ ergs s^{-1}, whereas the core components have luminosities of $5.8 \times 10^{33}(d_{10\,\mathrm{kpc}})^2$ ergs s^{-1} on October 15/16, respectively. Using the observed (scattered) sizes of the compact cores yields minimum brightness temperatures of 1.7×10^9 K (October 10) and 2.2×10^8 K (October 15/16). The corresponding sizes are 0.7 and 0.2 mas, respectively, if the intrinsic (unscattered) brightness temperatures are limited by the inverse-Compton effect. These numbers define a lower limit to the core magnetic fields B_c of order 10^{-3} G. Upper limits as given by the scattered sizes are 0.8 and 50 G, respectively.

Crude estimates of the frequency ν_{max} at which the flux density of the secondary components peak may be obtained as follows. With the assumptions that the corresponding magnetic fields are higher than the 3 K equivalent magnetic field of about 10^{-6} G, that the equipartition magnetic field is 8×10^{-5} G, and that the spectrum is optically thin [$\alpha = -0.7$, $S(\nu) \approx \nu^{+\alpha}$], we obtain $\nu_{\mathrm{max}} \approx 300$ MHz. The corresponding

synchrotron (half-)lifetimes of relativistic electrons, 17,000 yr, shows energy loss due to synchrotron radiation to be unimportant for the observed source sizes of the ejected components given the above assumptions are correct. The upper limit for the magnetic field in the core, $B_c = 50$ G, suggests lifetimes in excess of $1.03/(\nu_{max})^{1/2}$ (GHz) days and is relatively insensitive to ν_{max}, which does not contribute more than a factor of 10 between 30 GHz and 300 MHz.

The multifrequency monitoring of the total emission of the source shows that the turnover frequency is lower than 1.5 GHz for the optically thin events. This strengthens the assumption made above that the turnover frequency is about 300 MHz.

4.3. *The Distance to Cygnus X-3*

The combination of observations of the large outburst on October 10 and the detection of substructure with a resolution at the scattering limit can be used to estimate an upper limit of the distance to Cygnus X-3 as follows.

The duration of the outburst at 6 cm wavelength as given by the logarithmic timescale $\tau = \langle S \rangle (d\tau/dS)$ is 2.75 days, corresponding to a light-travel time size of 7.1×10^{15} cm. This is consistent with the (logarithmic) timescale of the variability of the core component at 6 cm (3.05 days) and is also evident in the light curve at 11.1 cm (see Fig. 1).

An angular size of 1 mas corresponds to $1.5 \times 10^{13} d_{kpc}$ cm. Since the simplest kinematic model of the October 10 outburst is that of a source expansion consistent with the VLBI structure observed on October 15/16, i.e., expanding to 30 mas on each side, an estimate for the distance based on light-travel time gives a distance of 15 kpc.

As the velocity during the outburst must be less than c, the source size is underestimated. We regard our result of 15 kpc as a conservative upper limit of the distance to Cygnus X-3. From H I absorption-line measurements, Dickey (1983) derives lower limits to Cygnus X-3 in the range 11.6–12.8 kpc $\times \pi_0$ (the galactocentric radius in kpc). With the revised distance to the Galactic center of 7 kpc (Reid et al. 1988), the lower limit to the distance of Cygnus X-3 is 8–9 kpc. For convenience we normalize our calculation of source parameters to 10 kpc.

5. SUMMARY

Observations of Cygnus X-3 with the European VLBI Network at a wavelength of 6 cm during the 1985 October outburst have led to the following results.

The milliarcsecond structure at two epochs is found to be consistent with a compact central core and a bidirectional jet of about 60 mas in size. The identification of individual outbursts as the onset of a linear expansion together with the source morphology yields an expansion velocity of $0.3c \times d_{10\,kpc}$. The data are consistent with an intrinsic jet velocity $\beta = 0.3$. Scattering diameter and inverse-Compton sizes define the extreme values of possible core magnetic fields to be in the range of 10^{-3} to 50 G.

Furthermore, the measurements of Cygnus X-3 during a quiescent period in 1985 May 21 and 23 are consistent with a compact source (23 ± 2 mas) where the size is within the error bars of the weighted average of the scatter-broadened image (16 ± 6 mas) observed during the 1985 October flare.

The detection of VLBI structure as well as the comparable timescales of core and total flux density variability allow us to put an upper limit on the distance to Cygnus X-3 of 15 kpc and thus confirm the Galactic origin of the source.

The image is consistent with a complex source whose individual components are dominated by interstellar scattering, with a scattering size of 16 ± 6 mas at 6 cm. Using previously published scattering sizes at lower frequencies in addition, we derive a frequency dependence of $\theta \approx \nu^{-2.07 \pm 0.04}$. The corresponding spectral index 3.87 ± 0.07 is slightly in excess of the Kolmogorov value (11/3) for neutral turbulence.

The measured value of $L\langle C_n^2 \rangle = 10.7_{kpc\,m} - 20/3$ confirms enhanced scattering toward the line of sight to Cygnus X-3, because of interstellar matter in the Cygnus region. This scattering may occur in a medium very close to Cygnus X-3.

Although the observations of the 1985 October outburst are the first direct detection of symmetrical jetlike features in Cygnus X-3 separating from a central core, details of the kinematics remain to be studied by further high-resolution observations. Future studies should focus on the investigation of a possible precession of milliarcsecond jetlike features, in order to constrain physical models of the binary system. SS 433 shows precession on the order of 162 days, which is roughly 10 times the orbital period, in the radio as well as in the optical data (e.g., Hjellming & Johnston 1986). In the case of Cygnus X-3 only VLBI observations (during outbursts) can reveal a possible precession of the jetlike structures. Due to scattering and the rapid expansion of the source, the EVN with its sensitive baselines to Effelsberg, operating at wavelengths shorter than 6 cm, is the appropriate array to observe this source, beginning with a delay of about 1 day after the onset of a big outburst to be followed by high dynamic range observations with the MERLIN array.

To obtain information about the central radio source, higher frequency VLBI observations have to be performed. The predicted scattering size of Cygnus X-3 at 90 GHz of 0.04 mas is comparable to the inverse-Compton size of 0.01–0.04 mas extrapolated from the 6 cm VLBI data (assuming flat spectrum and frequency independence of brightness temperatures and that the radio emission is entirely due to incoherent synchrotron processes). Since the resolution of a global VLBI array operating at 90 GHz is 0.06 mas, any detection of fringes during an outburst of several janskys would be indicative of a compact source radiating at the 10^{12} K limit. A reliable nondetection would place a lower limit on the source size and thus constrain physical parameters of the central region. The first observations of Cygnus X-3 at 90.9 and 230 GHz, obtained with the 30 m millimeter-wave telescope at Pico Veleta, Spain, between 1985 October 6 and October 8 (Baars et al. 1986), show evidence for a variability timescale on the order of 1 hr, which translates into a source size of ≤ 0.7 mas, comparable to the derived 10^{12} K brightness temperature inferred size at 6 cm.

It is a pleasure to thank the chairman of the European VLBI Network program committee and the VLBI Network for the allocation of ad hoc VLBI observing time; the interferometer staff at Green Bank for help with the observations; and W. J. Altenhoff, A. Alberdi, C. A. Hummel, T. P. Krichbaum, and A. Quirrenbach for fruitful discussions.

REFERENCES

Alef, W., & Porcas, R. W. 1986, A&A, 168, 365
Anderson, B., Conway, R. G., Davis, R. J., Peckman, R. J., Richards, P. J., Spencer, R. E., & Wilkinson, P. N. 1972, Nature Phys. Sci., 239, 117
Baars, J. W. M., Altenhoff, W. J., Hein, H., & Steppe, H. 1986, Nature, 324, 39
Becklin, E. E., Kristian, J., Neugebauer, G., & Wynn-Williams, C. G. 1972, Nature, 239, 130
Brinkman, A., Parsignault, D., Giaconni, R., Gursky, H., Kellogg, E., Schreier, E., & Tananbaum, H. 1972, IAU Circ., No. 2446
Cordes, J. M., Ananthakrishnan, S., & Dennison, B. 1984, Nature, 309, 689
Cordes, J. M., Pidwerbetsky, A., & Lovelace, R. V. E. 1986, ApJ, 310, 737
Cordes, J. M., Weisberg, J. N., & Boriakoff, V. 1985, ApJ, 288, 221
Davidsen, A., & Ostriker, J. P. 1974, ApJ, 189, 331
Diamond, P. J., Martinson, A., Dennison, B., Booth, R. S., & Winnberg, A. 1988, in Radio Wave Scattering in the Interstellar Medium, ed. J. M. Cordes (New York: AIP), 195
Dickey, J. M. 1983, ApJ, 273, L9
Fiedler, R. L., et al. 1987, ApJS, 65, 319
Geldzahler, B. J., et al. 1983, ApJ, 273, L65
Gregory, P. C., Kronberg, P. P., Seaquist, E. R., Hughes, V. A., Woodsworth, A., Viner, M. R., & Retallak, D. 1972, Nature, 239, 440
Gwinn, C. R., Moran, J. M., Reid, M. J., & Schneps, M. H. 1988, ApJ, 330, 817
Hjellming, R. M., & Johnston, K. J. 1986, in The Physics of Accretion onto Compact Objects, ed. K. O. Mason, M. G. Watson, & N. E. White, Lecture Notes in Physics, 266 (Berlin: Springer), 287
Johnston, K. J., Fiedler, R., Waltman, E., Spencer, R., & Hjellming, R. M. 1993, ApJ, submitted
Johnston, K. J., et al. 1986, ApJ, 309, 707
Marscher, A. P., & Brown, R. L. 1975, ApJ, 200, 719
Molnar, L. A., Reid, M. J., & Grindlay, J. E. 1984, Nature, 310, 662
———. 1985, in Radio Stars, ed. R. M. Hjellming & D. M. Gibson (Dordrecht: Reidel), 329
———. 1988, ApJ, 331, 494
Reid, M. J., Schneps, M. H., Moran, J. M., Gwinn, C. R., Genzel, R., Downes, D., & Rönnäng, B. 1987, ApJ, 330, 809
Spencer, R. E., Swinney, R. W., Johnston, K. J., & Hjellming, R. M. 1986, ApJ, 309, 694
Strom, R. G., van Paradijs, J., & van der Klis, M. 1989, Nature, 337, 234
van den Heuvel, E. P. J., & De Loore, C. 1973, A&A, 25, 387
Weekes, T. C., & Geary, J. C. 1982, PASP, 94, 708
Wilkinson, P. N., Spencer, R. E., & Nelson, R. F. 1988, in IAU Symp. 129, The Impact of VLBI on Astrophysics and Geophysics, ed. M. J. Reid & J. M. Moran (Dordrecht: Kluwer), 305